JOURNAL OF CHEMICAL & ENGINEERING DATA

ARTICLE

pubs.acs.org/jced

Vapor−Liquid Equilibrium Data for the Nitrogen + Dodecane System at Temperatures from (344 to 593) K and at Pressures up to 60 MPa

Tomás García-Córdova,[†] Daimler N. Justo-García,[‡] Blanca E. García-Flores,[†] and Fernando García-Sánchez*[,†]

[†]Laboratorio de Termodinámica, Programa de Investigación en Ingeniería Molecular, Instituto Mexicano del Petróleo, Eje Central Lázaro Cárdenas 152, 07730 México, D.F., México

[‡]Departamento de Ingeniería Química Petrolera, ESIQIE, Instituto Politécnico Nacional, Unidad Profesional Adolfo López Mateos, 07738 México, D.F., México

Supporting Information

ABSTRACT: A static-analytical apparatus with visual sapphire windows and pneumatic capillary samplers has been used to obtain new vapor−liquid equilibrium data for the $N_2 + C_{12}H_{26}$ system over the temperature range from (344 to 593) K and at pressures up to 60 MPa. Equilibrium phase compositions and vapor−liquid equilibrium ratios are reported. All of the measured vapor−liquid equilibrium data were subject to a thermodynamic consistency test of high-pressure vapor−liquid equilibrium data involving the calculation of the vapor-phase composition from the isothermal pressure liquid phase composition data. The consistency test showed that most of the data are thermodynamically consistent. The new results were compared with solubility data reported by other authors. The comparison showed that the vapor−liquid equilibrium data obtained in this study are in good agreement with those reported in the literature. The experimental data were modeled with the PR (Peng−Robinson) and PC-SAFT (perturbed-chain statistical associating fluid theory) equations of state by using one-fluid mixing rules and a single temperature-independent interaction parameter. Results of the modeling indicated that the PC-SAFT equation of state represents better the measured data of the $N_2 + C_{12}H_{26}$ system over the whole temperature, pressure, and composition range studied.

INTRODUCTION

The development of separation processes such as distillation, extraction, or absorption for the petroleum industry has required a lot of research to determine, generalize, and predict the vapor−liquid equilibria of hydrocarbon mixtures that rely on the operations to the petroleum industry. At present, there exists considerable information in the literature on the vapor−liquid equilibria of hydrocarbons at different conditions of temperature and pressure. This information has been used by the petroleum industry to develop equations of state able to predict correctly the vapor−liquid equilibria of hydrocarbons over wide temperature and pressure ranges.

In the case of the vapor−liquid equilibria of N_2-hydrocarbon binary mixtures, many studies on the solubility of N_2 in paraffin, aromatic, and naphthenic compounds have already been reported in the literature (see ref 1 and references therein); however, some of these studies have been performed over limited ranges of temperature and pressure.

On the other hand, knowledge of N_2 solubility in hydrocarbon compounds is important in relation to an optimal recovery strategy in enhanced oil recovery by N_2 injection at high pressure. Consequently, the treatment of these mixtures requires experimental information on the vapor−liquid equilibria at high pressure. However, this information is difficult to obtain because it is necessary for an apparatus to be able to stand high pressures and that allows accurate determinations of pressure and composition of the phases in equilibrium. Moreover, the information of the vapor−liquid equilibria at high pressures is necessary for the development and/or validation of theoretical models applicable to these systems.[2,3]

The phase behavior prediction of systems containing N_2 with hydrocarbons is a challenging task since all binary N_2 + hydrocarbon fluid mixtures develop, except for methane, type III phase diagrams according to the classification scheme of van Konynenburg and Scott,[4] which exhibit two distinct critical curves, one starting at the critical point of the component with the higher critical temperature that goes to infinite pressures, whereas the other critical curve starts at the critical point of the component with the lower critical temperature and meets a three-phase line of liquid−liquid−vapor at an upper critical end point. Therefore, it is important to carry out experimental phase equilibrium studies at elevated temperatures and pressures of N_2-containing binary systems along with some modeling effort using thermodynamic models to give the right qualitative and quantitative description of the phase behavior of N_2-hydrocarbon mixtures and thus providing a better understanding of phase behavior patterns that hydrocarbon mixtures develop during an enhanced oil recovery process by high-pressure N_2 injection.

Special Issue: John M. Prausnitz Festschrift

Received: November 16, 2010
Accepted: January 18, 2011
Published: February 11, 2011

ACS Publications © 2011 American Chemical Society

To increase the experimental database of vapor−liquid equilibria for mixtures containing N_2 and a hydrocarbon, we have undertaken a systematic study of the phase behavior of N_2 + hydrocarbon mixtures at high pressures. Previously, we have reported vapor−liquid equilibrium data of N_2 + alkane (from pentane to decane) mixtures over wide temperature ranges and at pressures up to 50 MPa.[5−10] These studies are part of a research program where phase behavior is studied for enhanced oil recovery in selected Mexican fields by high-pressure N_2 injection.

In this work, we report new vapor−liquid equilibrium measurements for the system N_2 + $C_{12}H_{26}$ over the temperature range from (344 to 593) K and at pressures up to 60 MPa. Seven isotherms are reported in this study, which were determined in a high-pressure phase equilibrium apparatus of the static-analytical type using a sampling-analyzing process for determining the composition of the coexisting phases. All of the measured N_2 + $C_{12}H_{26}$ vapor−liquid equilibrium data were subject to a thermodynamic consistency test according to the method proposed by Christiansen and Fredenslund.[11]

The experimental data obtained in our measurements were correlated using the PR (Peng−Robinson)[12] and PC-SAFT (perturbed-chain statistical associating fluid theory)[13] equations of state. The mixing rules used for these equations were the classical one-fluid mixing rules. For both models, a single temperature-independent interaction parameter was fitted to all experimental data.

EXPERIMENTAL SECTION

Materials. N_2 and He (carrier gas) were acquired from Aga Gas (Mexico) and Infra (Mexico), respectively, both with a certified purity greater than 0.99999 in mole fraction. Dodecane ($C_{12}H_{26}$) was purchased from Aldrich (USA) with a gas−liquid chromatography (GLC) minimum purity of 0.99 in mole fraction. They were used without further purification except for the careful degassing of the $C_{12}H_{26}$.

Apparatus and Procedure. A detailed description of the experiment and methods used in this work has been reported earlier by García-Sánchez and coworkers.[5−7] Briefly, the apparatus consists mainly of an equilibrium cell, a sampling-analyzing system, a pressure transducer, two platinum temperature sensors, a magnetic stirring device, a timer, and compressed-air control device for each sampler, an analytical system, and feeding and degassing circuits. This apparatus is based on the static-analytical method with fluid phase sampling and can be used to determine the multiphase equilibrium of binary and multicomponent systems between (313 and 673) K and at pressures up to 60 MPa.

The equilibrium cell (made of titanium) has an internal volume of about 100 mL and holds two sapphire windows for visual observation. The cap of the cell, used for studies at high temperatures with up to three coexisting phases, holds the three sampling systems with capillaries of different lengths: the extremity of one capillary is at the top of the cell (vapor withdrawing), another one at the bottom of the cell (withdrawing of the dense liquid), and the third one in an intermediate position (light liquid phase withdrawing). The sampling-analyzing system is constituted of three capillary samplers[14] connected altogether online with a gas chromatograph, which makes the apparatus very practical and accurate for measurements at high temperatures and pressures. The equilibrium cell can be maintained within ± 0.2 K for temperatures between (313 and 673) K by means of a high-temperature regulating air thermostat.

Temperature measurements in the equilibrium cell were monitored by using two Pt100 resistance thermometers, which are periodically calibrated against a 25 Ω reference platinum resistance (Tinsley Precision Instruments, UK). The resulting uncertainty of the two Pt100 probes is, usually, not higher than ± 0.02 K; however, drift in the temperature of the air oven makes the uncertainty of the temperature measurements to be ± 0.2 K. Pressure measurements were carried out by means of a pressure transducer (Sensonetics for temperatures up to 673 K), which is periodically calibrated against a dead-weight pressure balance. Pressure measurement uncertainties are estimated to be within ± 0.02 MPa for pressures up to 60 MPa.

The analytical work was carried out using a gas chromatograph (Varian 3800) equipped with a thermal conductivity detector (TCD), which is connected to a data acquisition system (Star GC Workstation, Ver. 5.3). The analytical column used is a Restek 3 % RTX-5 column (mesh 100/120 Silcoport-W, silcosteel tube, length: 1.83 m, diameter: 3.175 mm). The TCD was used to detect the $C_{12}H_{26B}$ and N_2 compounds. It was calibrated by injecting known amounts of $C_{12}H_{26}$ and N_2 through liquid-tight (5 μL) and gas-tight (1000 μL) syringes, respectively. Calibration data were fitted to a straight line, leading to an estimated mole fraction uncertainty less than 1 % for liquid and vapor phases on the whole concentration range.

Once the pressure transducer, platinum temperature probes, and chromatographic thermal conductivity detector have been calibrated, the system was preflushed with isopropyl alcohol and then dried under vacuum at 423 K. After drying under vacuum, the system was purged with N_2 to ensure that the last traces of solvents were removed. During an experimental run, the liquid component, previously degassed according to the method of Battino et al.,[15] is first introduced into the cell. The equilibrium cell and its loading lines are evacuated before filling it with the degassed liquid component. Once the desired temperature is reached and stabilized, the gaseous component, previously stored in a high-pressure cell, is carefully introduced into the equilibrium cell until the pressure of measurement. Then the magnetic stirring device is activated to reach equilibrium, which is indicated by pressure stabilization. Pressure is adjusted by injecting again the gaseous component and acting the stirring device until reaching the desired pressure. After the equilibrium in the cell is achieved, measurements are performed using the capillary-sampling injectors, which are connected to the equilibrium cell by 0.1 mm internal diameter capillary tubes of different lengths. The samples are injected and vaporized directly into the carrier gas (He) stream of the gas chromatograph. For each equilibrium condition, at least 25 equilibrium samples are withdrawn using the pneumatic samplers and analyzed to check for measurement and repeatability. As the volume of the withdrawn samples is very small compared to the volume of the vapor or liquid present in the equilibrium cell, it is possible to withdraw many samples without disturbing the phase equilibrium. To avoid condensation and adsorption of the $C_{12}H_{26}$, the samplers and all of the lines for the gas stream are superheated to ensure that the whole of the samples is transferred to the chromatograph.

RESULTS

The N_2 + $C_{12}H_{26}$ system has been previously studied by D'Avila et al.,[16] Ampueda Ramos,[17] Llave and Chung,[18] and Gao et al.[19] at different temperature and pressure conditions. Table 1 contains a summary of the earlier results, including those

Table 1. Summary of Vapor−Liquid Equilibria for the $N_2 + C_{12}H_{26}$ System

ref	T/K	p/MPa	no. of points	remarks
16	348.2−423.2	7.21−9.39	9	$p-y$ data
17	313.2−369.2	2.29−14.04	21	$p-x-y$ data
18	327.6−366.5	4.91−22.96	16	$p-x$ data
19	344.3−410.9	1.29−9.55	24	$p-x$ data
this work	344.4−593.5	0.55−60.06	169	$p-x-y$ data

presented in this paper. The new measured phase equilibrium compositions for this binary system in terms of N_2 liquid and vapor mole fractions and their respective uncertainties, temperatures, and pressures are tabulated in Table 2. Average uncertainties in the phase compositions, due mainly to errors associated with sampling, are estimated to be ± 0.004 for the liquid phase and ± 0.001 for the vapor phase, in the mole fraction over the whole concentration range.

From chromatographic measurements, mole fractions z_i are calculated through the expression

$$z_i = \frac{1}{1 + \sum_{j \neq i} R_{ij} S_{ji}} \qquad z_i = x_i \text{ or } y_i \tag{1}$$

and uncertainties on mole fractions through eq 2

$$\Delta z_i = z_i^2 \sum_{j \neq i} (R_{ij} \Delta S_{ji} + S_{ji} \Delta R_{ij}) \tag{2}$$

where $R_{ij} = R_i/R_j$ is the ratio of the response coefficients R_i and R_j, $S_{ij} = S_j/S_i$ is the ratio of the chromatographic peak areas S_j and S_i, ΔS_{ij} is estimated by means of the varying results of analyses on at least 10 samples, and ΔR_{ij} is the mean quadratic deviation in mole number for components i and j, resulting from a data fitting on the results of the chromatographic detector calibration.

Table 2 also presents the vapor pressures of $C_{12}H_{26}$ at each temperature level. These values were calculated with the Frost−Kalkwarf[20] equation using the parameters reported by Reid et al.[21] as follows

$$p_{vp}/\text{MPa} = 0.1 \exp[77.628 - 10012.5/(\text{K}/T) - 9.236 \ln(T/\text{K}) + 100300(p_{vp}/\text{MPa})/(\text{K}/T)^2] \tag{3}$$

where p_{vp} is the vapor pressure and T is the temperature. Since p_{vp} appears on both sides of eq 3, then it should be solved iteratively for p_{vp} by using, for instance, the Wegstein method,[22] which converges in a few iterations.

The calculated K values, defined as the equilibrium ratio between the vapor and the liquid for each component at a given temperature and pressure, are also given in Table 2. This table shows that, for all of the isotherms studied, N_2 has K values higher than one whereas $C_{12}H_{26}$ has K values lower than the unity, which indicates that the N_2 concentrates in the vapor phase whereas $C_{12}H_{26}$ does it in the liquid phase.

Figure 1 shows the experimental solubilities of N_2 in the $C_{12}H_{26}$-rich liquid phase on a pressure−composition diagram at (344.4 and 410.7) K along with the solubility results of Ampueda Ramos,[17] Llave and Chung,[18] and Gao et al.[19] at about the same temperatures. This figure shows that our experimental results at 344.4 K are in good agreement with those determined by Gao et al. but differ from those reported by the other authors. Good agreement is also found between our experimental data and those reported by Gao et al. at 410.9 K.

Table 2. Experimental Vapor−Liquid Equilibrium Data for the N_2 (1) + $C_{12}H_{26}$ (2) System at Different Temperatures[a]

p/MPa	x_1	± Δx_1	y_1	± Δy_1	K_1	K_2
			T/K = 344.4			
0.0005[b]	0.0000		0.0000			
1.43	0.0204	0.0005	0.9987	0.0001	48.9559	0.0013
2.90	0.0411	0.0009	0.9992	0.0001	24.3114	0.0008
5.03	0.0669	0.0015	0.9994	0.0001	14.9387	0.0006
7.52	0.0952	0.0023	0.9995	0.0001	10.4989	0.0006
9.76	0.1182	0.0025	0.9995	0.0001	8.4560	0.0006
12.38	0.1435	0.0029	0.9995	0.0001	6.9652	0.0006
15.26	0.1703	0.0029	0.9994	0.0001	5.8685	0.0007
17.51	0.1881	0.0031	0.9994	0.0001	5.3131	0.0007
19.97	0.2098	0.0038	0.9993	0.0001	4.7631	0.0009
22.52	0.2280	0.0040	0.9992	0.0001	4.3825	0.0010
24.88	0.2438	0.0041	0.9992	0.0001	4.0984	0.0011
27.49	0.2588	0.0039	0.9991	0.0001	3.8605	0.0012
29.58	0.2716	0.0043	0.9991	0.0001	3.6786	0.0012
32.42	0.2908	0.0043	0.9990	0.0001	3.4354	0.0014
35.03	0.3032	0.0047	0.9989	0.0001	3.2945	0.0016
37.65	0.3170	0.0047	0.9988	0.0001	3.1508	0.0018
39.98	0.3314	0.0048	0.9987	0.0001	3.0136	0.0019
42.26	0.3407	0.0049	0.9986	0.0002	2.9310	0.0021
45.09	0.3572	0.0052	0.9985	0.0001	2.7954	0.0023
47.33	0.3665	0.0053	0.9984	0.0001	2.7241	0.0025
50.20	0.3771	0.0050	0.9983	0.0002	2.6473	0.0027
52.60	0.3890	0.0052	0.9982	0.0002	2.5661	0.0029
55.02	0.3991	0.0054	0.9981	0.0002	2.5009	0.0032
57.50	0.4095	0.0055	0.9980	0.0001	2.4371	0.0034
60.04	0.4190	0.0053	0.9978	0.0001	2.3814	0.0038
			T/K = 410.7			
0.0098[b]	0.0000		0.0000			
1.14	0.0184	0.0006	0.9915	0.0003	53.8859	0.0087
2.17	0.0339	0.0007	0.9949	0.0002	29.3466	0.0053
3.13	0.0483	0.0011	0.9959	0.0002	20.6190	0.0043
3.93	0.0596	0.0013	0.9965	0.0002	16.7190	0.0038
5.02	0.0754	0.0018	0.9969	0.0002	13.2215	0.0034
7.57	0.1089	0.0022	0.9974	0.0001	9.1586	0.0030
10.14	0.1383	0.0027	0.9974	0.0001	7.2121	0.0030
12.98	0.1698	0.0030	0.9973	0.0001	5.8733	0.0033
14.83	0.1890	0.0034	0.9972	0.0001	5.2762	0.0035
17.53	0.2158	0.0037	0.9970	0.0001	4.6200	0.0038
20.24	0.2426	0.0041	0.9968	0.0001	4.1087	0.0043
22.45	0.2653	0.0044	0.9966	0.0001	3.7565	0.0046
24.93	0.2879	0.0046	0.9964	0.0001	3.4609	0.0051
27.47	0.3091	0.0047	0.9961	0.0002	3.2225	0.0057
29.97	0.3313	0.0048	0.9959	0.0001	3.0060	0.0061
32.51	0.3508	0.0050	0.9956	0.0002	2.8381	0.0068
35.07	0.3698	0.0050	0.9951	0.0001	2.6908	0.0078
37.48	0.3903	0.0053	0.9948	0.0002	2.5487	0.0086
39.94	0.4109	0.0052	0.9943	0.0002	2.4198	0.0097
42.56	0.4298	0.0054	0.9938	0.0002	2.3122	0.0109
45.02	0.4469	0.0055	0.9934	0.0002	2.2229	0.0119
47.59	0.4600	0.0056	0.9929	0.0002	2.1585	0.0131
50.03	0.4760	0.0055	0.9923	0.0002	2.0847	0.0147

dx.doi.org/10.1021/je1012372 |J. Chem. Eng. Data 2011, 56, 1555–1564

Table 2. Continued

p/MPa	x_1	$\pm \Delta x_1$	y_1	$\pm \Delta y_1$	K_1	K_2
52.54	0.4917	0.0054	0.9918	0.0002	2.0171	0.0161
55.02	0.5062	0.0056	0.9911	0.0003	1.9579	0.0180
57.43	0.5205	0.0052	0.9906	0.0002	1.9032	0.0196
60.05	0.5341	0.0054	0.9899	0.0003	1.8534	0.0217
			T/K = 463.9			
0.0529[b]	0.0000		0.0000			
1.09	0.0202	0.0005	0.9501	0.0011	47.0347	0.0509
2.05	0.0372	0.0008	0.9710	0.0007	26.1022	0.0301
3.03	0.0544	0.0013	0.9790	0.0005	17.9963	0.0222
4.08	0.0716	0.0016	0.9831	0.0005	13.7304	0.0182
5.04	0.0875	0.0019	0.9853	0.0004	11.2606	0.0161
7.52	0.1245	0.0024	0.9878	0.0004	7.9341	0.0139
9.95	0.1593	0.0030	0.9888	0.0003	6.2072	0.0133
12.50	0.1945	0.0033	0.9894	0.0003	5.0869	0.0132
15.01	0.2272	0.0037	0.9895	0.0003	4.3552	0.0136
17.56	0.2568	0.0041	0.9894	0.0003	3.8528	0.0143
20.05	0.2868	0.0043	0.9891	0.0003	3.4487	0.0153
22.51	0.3150	0.0046	0.9885	0.0003	3.1381	0.0168
25.02	0.3439	0.0046	0.9879	0.0003	2.8726	0.0184
27.54	0.3706	0.0050	0.9874	0.0004	2.6643	0.0200
30.03	0.3965	0.0051	0.9867	0.0004	2.4885	0.0220
32.59	0.4194	0.0053	0.9859	0.0005	2.3507	0.0243
35.09	0.4415	0.0053	0.9850	0.0005	2.2310	0.0269
37.54	0.4653	0.0050	0.9836	0.0004	2.1139	0.0307
40.16	0.4877	0.0054	0.9826	0.0004	2.0148	0.0340
42.51	0.5092	0.0053	0.9815	0.0005	1.9275	0.0377
45.09	0.5318	0.0052	0.9803	0.0005	1.8434	0.0421
47.55	0.5487	0.0051	0.9786	0.0005	1.7835	0.0474
50.07	0.5661	0.0051	0.9773	0.0006	1.7264	0.0523
52.54	0.5847	0.0051	0.9758	0.0006	1.6689	0.0583
55.23	0.6018	0.0051	0.9738	0.0007	1.6181	0.0658
57.57	0.6188	0.0050	0.9717	0.0007	1.5703	0.0742
60.06	0.6338	0.0050	0.9701	0.0008	1.5306	0.0816
			T/K = 503.4			
0.1395[b]	0.0000		0.0000			
1.09	0.0213	0.0005	0.8680	0.0025	40.7512	0.1349
2.16	0.0436	0.0009	0.9272	0.0015	21.2661	0.0761
3.20	0.0639	0.0019	0.9469	0.0011	14.8185	0.0567
4.21	0.0834	0.0017	0.9568	0.0010	11.4724	0.0471
5.31	0.1041	0.0020	0.9628	0.0009	9.2488	0.0415
7.44	0.1403	0.0027	0.9696	0.0008	6.9109	0.0354
10.04	0.1837	0.0032	0.9728	0.0006	5.2956	0.0333
12.44	0.2213	0.0037	0.9746	0.0007	4.4040	0.0326
15.02	0.2602	0.0039	0.9755	0.0006	3.7490	0.0331
17.51	0.2945	0.0044	0.9754	0.0006	3.3121	0.0349
20.03	0.3252	0.0047	0.9753	0.0006	2.9991	0.0366
22.45	0.3592	0.0050	0.9743	0.0006	2.7124	0.0401
25.03	0.3927	0.0050	0.9735	0.0006	2.4790	0.0436
27.55	0.4223	0.0052	0.9720	0.0007	2.3017	0.0485
30.05	0.4526	0.0052	0.9708	0.0007	2.1449	0.0533
32.53	0.4828	0.0053	0.9692	0.0007	2.0075	0.0596
35.08	0.5089	0.0052	0.9674	0.0008	1.9010	0.0664
37.55	0.5353	0.0056	0.9653	0.0009	1.8033	0.0747
40.07	0.5587	0.0054	0.9625	0.0009	1.7227	0.0850

Table 2. Continued

p/MPa	x_1	$\pm \Delta x_1$	y_1	$\pm \Delta y_1$	K_1	K_2
42.61	0.5824	0.0052	0.9595	0.0009	1.6475	0.0970
45.07	0.6044	0.0051	0.9561	0.0010	1.5819	0.1110
47.54	0.6293	0.0051	0.9526	0.0012	1.5137	0.1279
50.05	0.6519	0.0060	0.9476	0.0012	1.4536	0.1505
52.52	0.6764	0.0050	0.9427	0.0014	1.3937	0.1771
55.11	0.7065	0.0045	0.9358	0.0015	1.3246	0.2187
57.50	0.7333	0.0044	0.9251	0.0018	1.2616	0.2808
59.26	0.7658	0.0040	0.9088	0.0021	1.1867	0.3894
			T/K = 532.9			
0.2569[b]	0.0000		0.0000			
0.94	0.0167	0.0008	0.7162	0.0031	42.8862	0.2886
1.17	0.0222	0.0005	0.7680	0.0039	34.5946	0.2373
1.54	0.0310	0.0008	0.8236	0.0031	26.5677	0.1820
2.03	0.0423	0.0010	0.8627	0.0026	20.3948	0.1434
3.03	0.0647	0.0014	0.8981	0.0019	13.8810	0.1089
4.02	0.0858	0.0017	0.9199	0.0016	10.7214	0.0876
5.03	0.1071	0.0020	0.9316	0.0014	8.6984	0.0766
6.01	0.1271	0.0024	0.9382	0.0013	7.3816	0.0708
7.28	0.1521	0.0028	0.9454	0.0012	6.2156	0.0644
9.95	0.2021	0.0034	0.9519	0.0011	4.7100	0.0603
12.45	0.2462	0.0040	0.9558	0.0010	3.8822	0.0586
15.28	0.2957	0.0043	0.9584	0.0010	3.2411	0.0591
17.51	0.3328	0.0052	0.9584	0.0010	2.8798	0.0624
19.95	0.3654	0.0049	0.9586	0.0011	2.6234	0.0652
22.49	0.4042	0.0055	0.9571	0.0016	2.3679	0.0720
25.03	0.4390	0.0054	0.9550	0.0013	2.1754	0.0802
27.56	0.4708	0.0057	0.9519	0.0015	2.0219	0.0909
30.04	0.5060	0.0053	0.9482	0.0014	1.8739	0.1049
32.51	0.5317	0.0053	0.9457	0.0014	1.7786	0.1160
35.43	0.5712	0.0057	0.9404	0.0015	1.6464	0.1390
37.58	0.5973	0.0052	0.9347	0.0015	1.5649	0.1622
40.07	0.6317	0.0049	0.9261	0.0016	1.4660	0.2007
42.46	0.6674	0.0047	0.9171	0.0017	1.3741	0.2492
45.10	0.7073	0.0044	0.8981	0.0023	1.2698	0.3481
46.38	0.7417	0.0043	0.8842	0.0026	1.1921	0.4483
			T/K = 562.1			
0.437[b]	0.0000		0.0000			
0.55	0.0029	0.0001	0.1732	0.0030	59.7241	0.8292
1.27	0.0223	0.0006	0.6132	0.0053	27.4978	0.3956
2.13	0.0435	0.0011	0.7587	0.0041	17.4414	0.2523
3.07	0.0655	0.0014	0.8204	0.0033	12.5252	0.1922
4.13	0.0905	0.0019	0.8570	0.0028	9.4696	0.1572
4.99	0.1099	0.0021	0.8775	0.0024	7.9845	0.1376
5.96	0.1315	0.0025	0.8908	0.0022	6.7741	0.1257
8.08	0.1778	0.0032	0.9067	0.0019	5.0996	0.1135
9.91	0.2166	0.0036	0.9165	0.0018	4.2313	0.1066
11.97	0.2582	0.0040	0.9208	0.0017	3.5662	0.1068
14.02	0.2982	0.0044	0.9236	0.0015	3.0973	0.1089
16.16	0.3384	0.0047	0.9247	0.0016	2.7326	0.1138
18.07	0.3743	0.0050	0.9245	0.0016	2.4699	0.1207
19.90	0.4055	0.0051	0.9241	0.0016	2.2789	0.1277
22.15	0.4435	0.0052	0.9216	0.0017	2.0780	0.1409
24.19	0.4816	0.0052	0.9191	0.0017	1.9084	0.1561
26.08	0.5131	0.0052	0.9127	0.0018	1.7788	0.1793

dx.doi.org/10.1021/je1012372 |*J. Chem. Eng. Data* 2011, 56, 1555–1564

Table 2. Continued

p/MPa	x_1	$\pm \Delta x_1$	y_1	$\pm \Delta y_1$	K_1	K_2
28.31	0.5497	0.0054	0.9046	0.0018	1.6456	0.2119
29.80	0.5769	0.0051	0.8990	0.0018	1.5583	0.2387
31.94	0.6215	0.0050	0.8874	0.0022	1.4278	0.2975
33.84	0.6612	0.0047	0.8729	0.0024	1.3202	0.3751
34.74	0.6862	0.0047	0.8592	0.0026	1.2521	0.4487
34.96	0.6991	0.0045	0.8490	0.0029	1.2144	0.5018
			T/K = 593.5			
0.726[b]	0.0000		0.0000			
1.10	0.0131	0.0004	0.2905	0.0044	22.1756	0.7189
2.27	0.0504	0.0011	0.5802	0.0051	11.5119	0.4421
3.28	0.0803	0.0016	0.6914	0.0045	8.6102	0.3355
4.21	0.1076	0.0022	0.7485	0.0040	6.9563	0.2818
5.07	0.1308	0.0024	0.7829	0.0035	5.9855	0.2498
7.09	0.1863	0.0032	0.8215	0.0031	4.4096	0.2194
8.96	0.2344	0.0039	0.8426	0.0029	3.5947	0.2056
10.96	0.2837	0.0043	0.8519	0.0027	3.0028	0.2068
13.13	0.3341	0.0047	0.8572	0.0026	2.5657	0.2144
14.86	0.3739	0.0049	0.8582	0.0027	2.2953	0.2265
17.26	0.4302	0.0051	0.8550	0.0028	1.9874	0.2545
19.07	0.4758	0.0052	0.8486	0.0027	1.7835	0.2888
21.02	0.5265	0.0053	0.8364	0.0029	1.5886	0.3455
22.03	0.5568	0.0052	0.8259	0.0031	1.4833	0.3928
23.24	0.6010	0.0050	0.8050	0.0033	1.3394	0.4887

[a] $\Delta T = \pm 0.2$ K; $\Delta p = \pm 0.02$ MPa. [b] Calculated vapor pressure of pure $C_{12}H_{26}$.

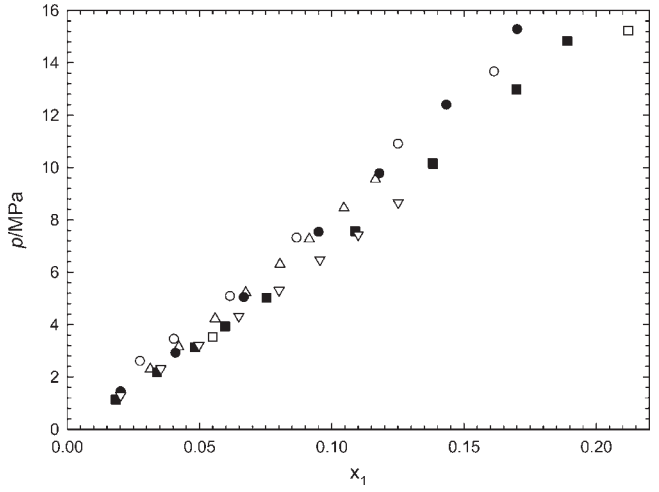

Figure 1. Experimental solubilities of N_2 (1) in $C_{12}H_{26}$ (2). This work: ●, 344.4 K; ■, 410.7 K. Ref 17: ○, 343.2 K. Ref 18: □, 344.3 K. Ref 19: △, 344.3 K; ▽, 410.9 K.

Figure 2 shows the results of the vapor−liquid equilibrium data obtained on a pressure−composition diagram for the seven experimental temperatures studied. In this figure, it can be observed that the solubility of N_2 in the $C_{12}H_{26}$-rich liquid phase increases as pressure increases for all isotherms investigated and that the solubility of N_2 in the $C_{12}H_{26}$-rich liquid phase decreases with decreasing temperature; that is, a trend of increasing solubility of N_2 in the $C_{12}H_{26}$-rich liquid phase is observed as temperature and pressure increase.

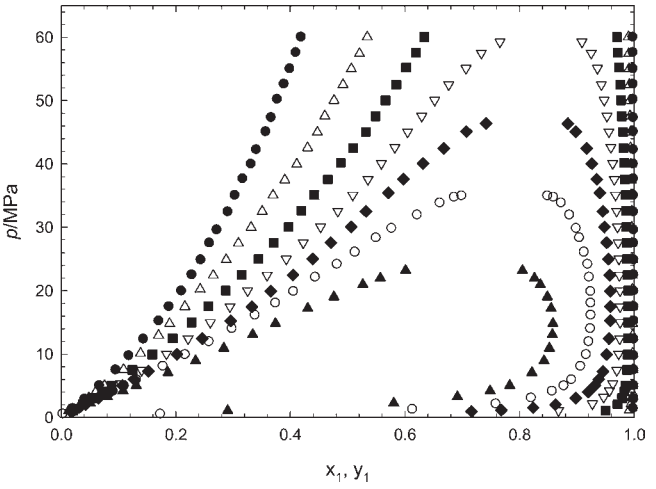

Figure 2. Experimental pressure−composition phase diagram for the N_2 (1) + $C_{12}H_{26}$ (2) system: ●, 344.4 K; △, 410.7 K; ■, 463.9 K; ▽, 503.4 K, ◆, 532.9 K, ○, 562.1 K; ▲, 593.5 K.

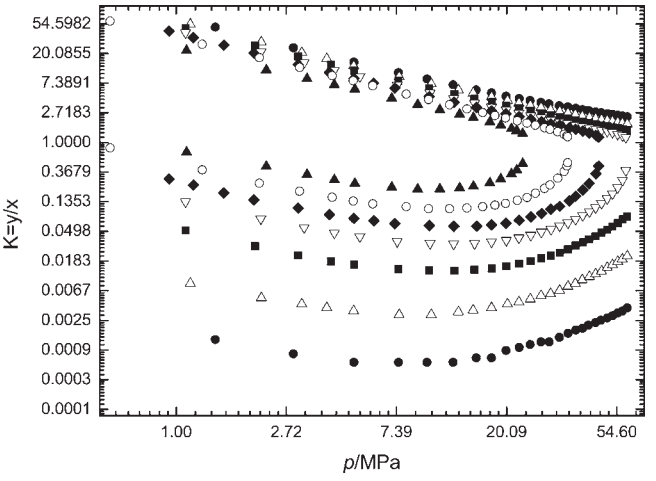

Figure 3. Effect of pressure on vapor−liquid equilibrium ratios for the N_2 (1) + $C_{12}H_{26}$ (2) system: ●, 344.4 K; △, 410.7 K; ■, 463.9 K; ▽, 503.4 K, ◆, 532.9 K, ○, 562.1 K; ▲, 593.5 K. N_2: K values higher than one; $C_{12}H_{26}$: K values lower than one.

Figure 3 shows the isotherms plotted in a log K value versus log p diagram. In this figure, there are two branches for each isotherm, one for each component, which will converge at the mixture critical point, where the K values are equal to the unity. The degree of smoothness of the curve for each isotherm reflects the internal consistency of the data; however, it is convenient to subject these data to a thermodynamic consistency test involving comparison between experimental and calculated vapor phase mole fractions by using either the procedure given by Christiansen and Fredenslund[11] or the one given by Won and Prausnitz.[23] Here, we have applied the method proposed by Christiansen and Fredenslund for testing the thermodynamic consistency of our measured data as shown below.

Isotherms obtained above the critical temperature of N_2 (T_c = 126.2 K) end up in the mixture critical point, which was approached by adding carefully small quantities of N_2 to avoid upsetting the phase equilibrium. After every step of adding N_2, the cell content was stirred at least two hours before withdrawing

dx.doi.org/10.1021/je1012372 |J. Chem. Eng. Data 2011, 56, 1555–1564

Table 3. Estimated Mixture Critical Data for the N_2 (1) + $C_{12}H_{26}$ (2) System

T/K	p/MPa	x_1	T/K	p/MPa	x_1
503.4	60.69	0.8626	593.5	24.13	0.6874
532.9	47.66	0.8196	658.0[a]	1.824[a]	0.0000
562.1	35.91	0.7670			

[a] Critical point of $C_{12}H_{26}$.[29]

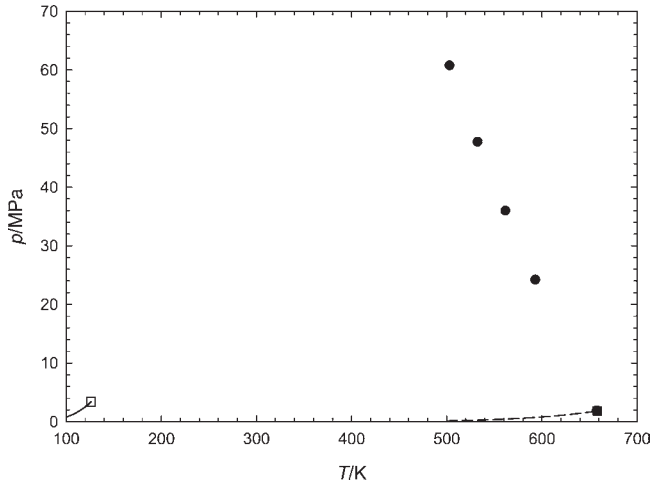

Figure 4. Pressure−temperature phase diagram for the N_2 + $C_{12}H_{26}$ system. This work: ●, mixture critical points. Ref 30: □, critical point of N_2; ref 29: ■, critical point of $C_{12}H_{26}$. —, vapor pressure of N_2; - - -, vapor pressure of $C_{12}H_{26}$.

the samples of the equilibrium phases. The measurements at (503.4, 532.9, 562.1, and 593.5) K and (59.26, 46.38, 34.96, and 23.24) MPa, respectively, were associated to an opalescence phenomenon, indicating the proximity of a critical state for this mixture. However, it was not possible to attain this terminal state due to that the apparatus is not suitable to measure this point directly. When the pressure was increased just above the critical point, only one phase was observed.

All isotherms studied in this work lie between the critical temperatures for the two components of this system. Since the equilibrium ratios for the two components converge to unity at the critical point of the mixture, it is then possible to obtain the critical pressure corresponding to each experimental temperature from the K values versus pressure diagram. Here, we estimated the mixture critical point for each isotherm by adjusting a series of pressure−composition data (all $p-x$ data and some $p-y$ data) to Legendre polynomials. Once having correlated these data, the pressure−composition phase diagram is calculated to locate the maximum pressure. For a system with two components, this maximum corresponds to the critical pressure of the mixture at constant temperature. The composition associated to this maximum pressure corresponds to the critical composition of the mixture. The estimated numerical values of the critical points for the N_2 + $C_{12}H_{26}$ system are reported in Table 3. At present, to our knowledge, no $p-T-x$ critical data has been reported in the literature for this system.

The mixture critical data reported in Table 3 were plotted in a pressure−temperature diagram shown in Figure 4. In this figure, the vapor−liquid coexistence region studied in this work is bounded by three lines: the vapor pressure curve of pure N_2, the vapor pressure curve of pure $C_{12}H_{26}$, and the mixture critical line (N_2 + $C_{12}H_{26}$). This figure also shows that, starting at the critical point of pure $C_{12}H_{26}$, the mixture critical line runs to lower temperatures and higher pressures exhibiting a positive curvature. The data displayed in Figure 4 allow suggesting that the system N_2 + $C_{12}H_{26}$ is a type III system according to the classification of van Konynenburg and Scott.[4] Nonetheless, to substantiate this claim, it is necessary to know how is the other critical line that departs from the critical point of pure N_2 and whether this system exhibits a three-phase line of liquid−liquid−vapor. However, we have no experimental evidence of these phase equilibrium phenomena for this system because they occur at low temperatures, and the apparatus used in this work is limited to be used at moderate and high temperatures. Moreover, because the melting point of $C_{12}H_{26}$ (263.6 K) is much higher than the critical temperature of N_2 (126.2 K), it is likely that a solid phase may appear in the system at the temperature around 126 K so that no liquid−liquid−vapor equilibrium can be observed.

THERMODYNAMIC CONSISTENCY OF THE DATA

The entire set of $p-x-y$ data at each isotherm for the N_2 + $C_{12}H_{26}$ system was subjected to the thermodynamic consistency test proposed by Christiansen and Fredenslund.[11] In this method, the vapor-phase composition in equilibrium with each experimental liquid-phase composition is calculated by the method of orthogonal collocation[24−26] within a thermodynamic framework which is internally consistent. The calculated vapor-phase compositions are compared with the experimental measured values, and if the absolute difference between the calculated and measured values is within the experimental error bounds, the data are considered to be thermodynamically consistent. A description of the consistency test method is given in Appendix A.

The results of the thermodynamic tests are given in Table 4, including the Henry's constant for N_2 in $C_{12}H_{26}$ calculated at each temperature. This table shows that, on the whole, the data are consistent according to the test, although the percentage of points passing the test decreases as temperature increases. Notwithstanding, since the experimental technique and the apparatus were the same for all temperatures, it is possible that some of the apparent lack of consistency at the higher temperatures may be caused by inadequacies in the method of calculating the fugacity coefficients, which were calculated from the PR[12] equation of state. Similar conclusions were reached by Kalra et al.[27] when subjected their vapor−liquid equilibrium data of the system N_2 + C_5H_{12} to the same thermodynamic test at temperatures from (277.4 to 377.6) K and at pressures up to 20.79 MPa. Table 4 shows that the calculated Henry's constant decrease as temperature increases.

Figure 5 shows the experimental vapor- and liquid-phase compositions in conjunction with the fitted pressure-liquid phase composition and the predicted pressure-vapor phase composition for the seven isotherms studied. In this figure it is seen that at low and moderate pressures the agreement between observed and calculated vapor is good, but it is lower as temperature and pressure increase, in particular close to the critical region for the isotherms at (503.4, 532.9, 562.1, and 593.5) K. This can be due to failure of the calculation of fugacity coefficients at high pressures and in the vicinity of the critical region. A possible solution to overcome this failure could be the appliance of a more theoretical equation of state (e.g., the PC-SAFT equation) to

Table 4. Consistency Test of N_2 (1) + $C_{12}H_{26}$ (2) Experimental Data and Henry's Constants, H_{12}, at Zero Pressure for N_2 (1) in $C_{12}H_{26}$ (2)

T/K	$(\Delta x + \Delta y)_{AVG}$[a]	$\lvert y(\text{exp}) - y(\text{calc})\rvert_{AVG}$	no. of exptl data points	no. of points passing test	H_{12}/ MPa
344.4	0.0040	0.0021	25	21	73.72
410.7	0.0042	0.0022	27	25	68.07
463.9	0.0045	0.0010	27	27	58.79
503.4	0.0051	0.0042	27	16	54.06
532.9	0.0054	0.0096	25	12	45.05
562.1	0.0060	0.0082	23	13	41.24
593.5	0.0070	0.0092	15	7	31.53
total number of data points			169	121	

[a] Average experimental uncertainty in liquid- and vapor-phase compositions.

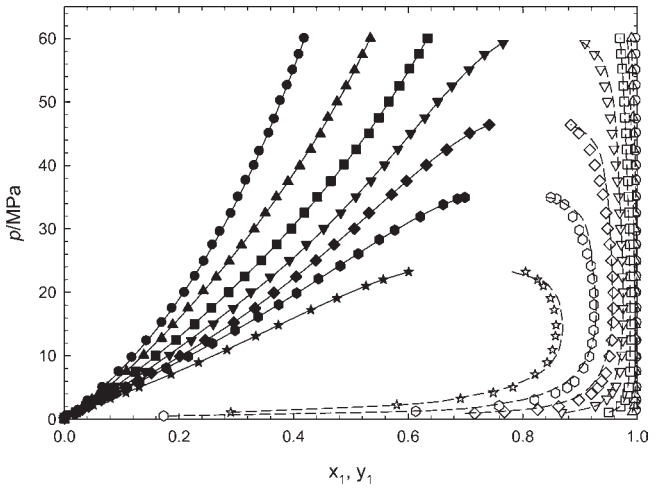

Figure 5. Pressure−temperature−composition diagram for N_2 (1) + $C_{12}H_{26}$ (2). $p-x_1$ data: ●, 344.4 K; ▲, 410.7 K; ■, 463.9 K; ▼, 503.4 K; ♦, 532.9 K; ⬢, 562.1 K; ★, 593.5 K. $p-y_1$ data: ○, 344.4 K; △, 410.7 K; □ 463.9 K; ▽, 503.4 K; ◇, 532.9 K; ⬡, 562.1 K; ☆, 593.5 K. Solid lines: $p-x_1$ data fitted to Legendre polynomials. Dashed lines: predicted vapor-phase composition.

calculate the fugacity coefficients and partial molar volume, instead of the PR equation.

MODELING

To predict the phase behavior of the $N_2 + C_{12}H_{26}$ system, we have estimated the interaction parameter for the PR[12] and PC-SAFT[13] equations of state by fitting the experimental vapor−liquid equilibrium data presented in Table 2 for this system. These equations of state were selected in this work due to their wide use for the calculation of vapor−liquid equilibria for fluid mixtures, including those mixtures encountered in the natural-gas and petroleum industries. The reader is referred to the original articles published by Peng and Robinson[12] and by Gross and Sadowski[13] for a detailed description of these equations of state.

The binary interaction parameter k_{ij} for the PR and PC-SAFT equations of state was estimated by minimizing the sum of squared relative deviations of bubble-point pressures and the sum of squared deviations in mole fraction of phase equilibrium compositions. The calculation of the phase equilibria was carried out by minimization of the Gibbs energy using stability tests (based on the tangent plane criterion) to find the most stable state of the system, according to the solution approach presented by Justo-García et al.[28] Critical properties (i.e., critical temperature T_c, critical pressure p_c, and critical volume V_c) and acentric factor ω of $C_{12}H_{26}$ for the PR equation of state were taken from Ambrose and Tsonopoulos[29] and from Ambrose,[30] respectively. Critical properties and acentric factor of N_2 were taken from Ambrose.[30] The three pure-component parameters (i.e., temperature-independent segment diameter σ, depth of the potential ε, and number of segments per chain m) of these compounds for the PC-SAFT equation of state were taken from Gross and Sadowski.[13]

The simplex optimization procedure of Nelder and Mead[31] was used in the computations by searching the minimum of the following objective functions:

$$S_1 = \sum_{i=1}^{M} \left[\left(\frac{p_i^{\text{exp}} - p_i^{\text{calc}}}{p_i^{\text{exp}}} \right)^2 + (y_i^{\text{exp}} - y_i^{\text{calc}})^2 \right] \quad (4)$$

for the bubble-point pressure method, and

$$S_2 = \sum_{i=1}^{M} [(x_i^{\text{exp}} - x_i^{\text{calc}})^2 + (y_i^{\text{exp}} - y_i^{\text{calc}})^2] \quad (5)$$

for the flash calculation method, where the terms $p_i^{\text{exp}} - p_i^{\text{calc}}$, $x_i^{\text{exp}} - x_i^{\text{calc}}$, and $y_i^{\text{exp}} - y_i^{\text{calc}}$ are the differences between the experimental and calculated values of, respectively, bubble-point pressures, liquid mole fractions, and vapor mole fractions for an experiment i, and M is the total number of experiments.

Once the minimization of objective functions S_1 and S_2 was performed, the agreement between calculated and experimental values was established through the standard percent relative deviation in pressure, σ_P, and standard percent deviation in mole fraction for the liquid, σ_x, and vapor, σ_y, phases of the lightest component,

$$\sigma_P = 100 \left[\frac{1}{M} \sum_{i=1}^{M} \left(\frac{p_i^{\text{exp}} - p_i^{\text{calc}}}{p_i^{\text{exp}}} \right)^2 \right]^{1/2} \quad (6)$$

$$\sigma_x = 100 \left[\frac{1}{M} \sum_{i=1}^{M} (x_i^{\text{exp}} - x_i^{\text{calc}})^2 \right]^{1/2} \quad (7)$$

$$\sigma_y = 100 \left[\frac{1}{M} \sum_{i=1}^{M} (y_i^{\text{exp}} - y_i^{\text{calc}})^2 \right]^{1/2} \quad (8)$$

where σ_P, σ_x, and σ_y were obtained with the optimal values of the binary interaction parameters, and they are given in Table 5. This table shows the correlative capabilities of the PR and PC-SAFT equations by using the van der Waals one-fluid mixing rules and a temperature-independent binary interaction parameter for the $N_2 + C_{12}H_{26}$ system. Overall, it can be said that the quality for correlating the experimental vapor−liquid equilibrium data of this binary system with the PC-SAFT equation is superior to that obtained with the PR equation. The fits of the PR and PC-SAFT equations of state to the $N_2 + C_{12}H_{26}$ system are shown in Figures 6 and 7, respectively.

Figure 6 shows that the PR equation fits the data well at low and moderate pressures, but it is less satisfactory when temperature and/or pressure increase. The fact that predictions at the different temperatures are not precise indicates that a temperature-dependent interaction parameter is necessary to adequately

Table 5. Estimated Binary Interaction Parameters for the N_2 (1) + $C_{12}H_{26}$ (2) System

PR equation of state				PC-SAFT equation of state			
k_{12}	σ_P	σ_x	σ_y	k_{12}	σ_P	σ_x	σ_y
Bubble-Point Pressure Method							
0.1561	10.9		2.0	0.1446	6.8		0.8
Flash Method							
0.1462	2.9		1.9	0.1457		1.9	0.9

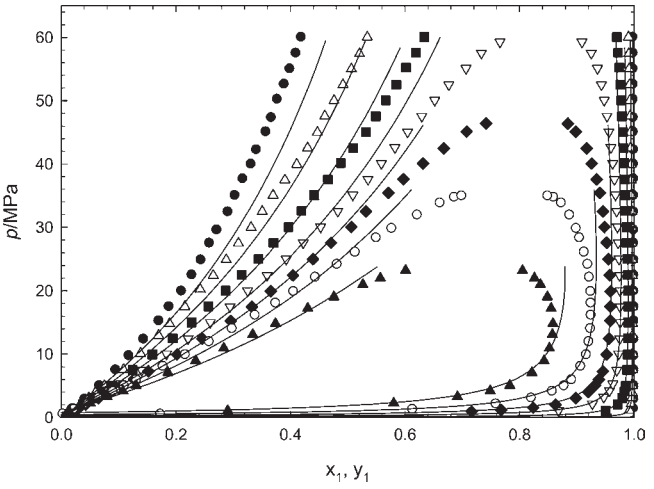

Figure 6. Experimental and calculated pressure−composition phase diagram for the N_2 (1) + $C_{12}H_{26}$ (2) system: ●, 344.4 K; △, 410.7 K; ■, 463.9 K; ▽, 503.4 K, ◆, 532.9 K, ○, 562.1 K; ▲, 593.5 K. Solid lines: PR EoS with k_{ij} = 0.1561 fitted to the VLE data of this work.

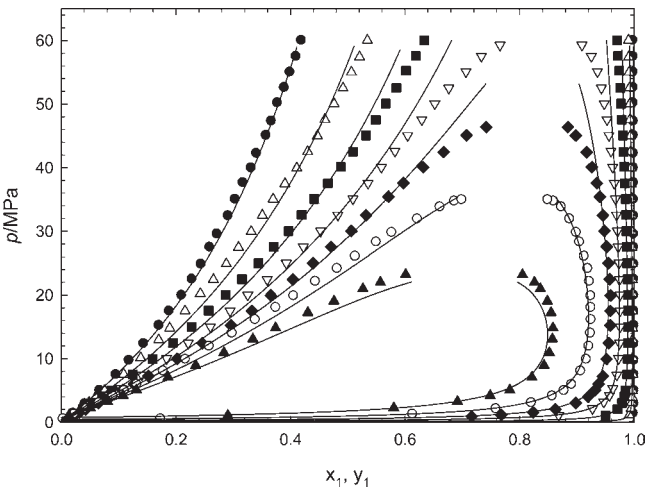

Figure 7. Experimental and calculated pressure−composition phase diagram for the N_2 (1) + $C_{12}H_{26}$ (2) system: ●, 344.4 K; △, 410.7 K; ■, 463.9 K; ▽, 503.4 K, ◆, 532.9 K, ○, 562.1 K; ▲, 593.5 K. Solid lines: PCSAFT EoS with k_{ij} = 0.1446 fitted to the VLE data of this work.

model the N_2 + $C_{12}H_{26}$ system when calculations are made over a wide range of temperatures. Nonetheless, this is outside the scope of this work, and no attempt was made to either determine this temperature dependence or apply other complex mixing rules or combining rules.

Figure 7 shows the results of the correlation with the PC-SAFT equation. In this figure, it can be seen that the overall agreement between experimental and calculated values is quite satisfactory, especially at highest temperatures. The superior quality of the PC-SAFT equation for predicting the phase behavior of asymmetric mixtures is due to that this model is based on a perturbation theory for chain molecules that can be applied to mixtures of small spherical molecules such as gases, nonspherical solvents, and chainlike polymers by using conventional one-fluid mixing rules.

Lastly, it should be mentioned that the parameters obtained from the correlation of the data with the PR and PC-SAFT equations do not reproduce, as most of the equations of state, the mixture critical points of this system.

CONCLUSIONS

New experimental vapor−liquid data have been obtained for the N_2 + $C_{12}H_{26}$ system at temperatures from (344 to 593) K and at pressures up to 60 MPa by using an experimental static-analytical apparatus with pneumatic capillary samplers. The smoothness of the equilibrium ratio−pressure curve for each isotherm showed suggests a low level of the random errors in the measurements. The estimated mixture critical data obtained from the vapor−liquid equilibrium measurements on this system suggest that it belongs to the type III class of systems according to the classification of van Konynenburg and Scott.

All of the experimental vapor−liquid data measured for the N_2 + $C_{12}H_{26}$ system over the temperature and pressures ranges studied were subjected to a consistency test based on the method of orthogonal collocation as proposed by Christiansen and Fredenslund. Results of the consistency test showed that most of the measured data (121 from 169) are thermodynamically consistent.

The PR and PC-SAFT equations of state with van der Waals one-fluid mixing rules were used to represent the measured data of this binary system by adjusting a single temperature-independent interaction parameter for each equation. Results of the representation showed that the PR equation fit the data well at low and moderate pressures but is less satisfactory at higher temperatures and/or pressures, while the PC-SAFT equation fit better the data over the whole temperature and pressure range studied.

APPENDIX A

Thermodynamic Consistency Test. All of the isothermal N_2 + $C_{12}H_{26}$ vapor−liquid equilibrium data presented in this work were subject to the thermodynamic consistency test proposed by Christiansen and Fredenslund.[11] The consistency test consists in calculating y_i from the isothermal $p-x$ data as described below.

Application of the isothermal, non-isobaric Gibbs−Duhem equation[32,33] to binary liquid systems in equilibrium with their vapors leads to the following relationship

$$p = y_1 p + y_2 p = \frac{x_1 f_1^{\circ} \gamma_1}{\varphi_1} + \frac{x_2 f_2^{\circ} \gamma_2}{\varphi_2} = \left(\frac{x_1 f_1^{\circ}}{\varphi_1}\right) \exp\left[g + x_2 \left(\frac{dg}{dx_1}\right)_{\sigma} - \left(\frac{x_2 V^{\mathrm{E}}}{RT}\right)\left(\frac{dp}{dx_1}\right)_{\sigma}\right] + \left(\frac{x_2 f_2^{\circ}}{\varphi_2}\right) \exp\left[g - x_1 \left(\frac{dg}{dx_1}\right)_{\sigma} + \left(\frac{x_1 V^{\mathrm{E}}}{RT}\right)\left(\frac{dp}{dx_1}\right)_{\sigma}\right] \quad \text{(A.1)}$$

where g is the reduced excess Gibbs energy, G^E/RT, V^E is the excess volume, f_i^o the reference fugacity, and φ_i the vapor phase fugacity coefficient of component i. In this equation, the subscript σ denotes "along the saturation line", and component 2 is the less volatile component.

Since N_2 (component 1) is a non-condensable component, then the reference fugacity for components 1 and 2 are given by

$$f_1^o = H_{1,2} \exp \int_{p_2^{sat}}^{p} \frac{\overline{V}_1^{\infty}}{RT} \, dp \quad (A.2)$$

and

$$f_2^o = p_2^{sat} \varphi_2^{sat} \exp \int_{p_2^{sat}}^{p} \frac{V_2}{RT} \, dp \quad (A.3)$$

respectively, whereas the excess volume is given by

$$V^E = V - x_1 \overline{V}_1^{\infty} - x_2 V_2 \quad (A.4)$$

where $H_{1,2}$ is Henry's constant, defined by

$$H_{1,2} = \lim_{x_1 \to 0} \left(\frac{y_1 \varphi_1 p}{x_1} \right) \quad (A.5)$$

Vapor-phase fugacity coefficients for pure components and mixtures are calculated from the PR[12] equation of state; liquid-phase molar volumes at saturation are calculated using the Lyckman−Eckert−Chueh correlation,[34,35] and the partial molar volume at infinite dilution $\overline{V}_1^{\infty}$ is obtained by differentiation of the PR equation of state.

The molar volume of the mixture is calculated from the Prausnitz−Chueh correlation,[34] who extended the Lyckman−Eckert−Chueh liquid-density correlation by taking into account the critical point problem.

When the properties φ_i, f_i^o, and V^E are available, eq A.1 can be solved for $g(x_1)$ as follows: First, it is necessary to represent the $p-x$ data analytically by using, for instance, Legendre polynomials according to the expression[36]

$$p - (1 - x_1')p_2^{sat} = x_1' \sum_{k=0}^{n} a_k L_k(x_1') \quad (A.6)$$

where $x_1' = x_1/x_{1,max}$ ($x_{1,max}$ being the largest value of x_1 in the data set), n is the highest order polynomial used, usually not higher than four, and $L_k(x_1)$ is the Legendre polynomial of degree k, given by

$$L_k(x_1) = (2k-1)(2x_1 - 1)L_{k-1}(x_1) - (k-1)L_{k-2}(x_1)/k$$
$$L_0(x_1) = 1 \qquad L_1(x_1) = 2x_1 - 1 \quad (A.7)$$

Equation A.7 is fitted to the $p-x$ data by using a least-squares technique.

Next, assuming that $g(x_1)$ may also be represented in terms of Legendre polynomials as

$$g = (x_1')^2 \sum_{k=0}^{n} a_k L_k[(x_1')^2] \quad (A.8)$$

where the polynomial coefficients are obtained by the method of orthogonal collocation as discussed by Christiansen and Fredenslund. In this case, the problem of solving the differential equation is reduced to solving n nonlinear algebraic equations in n unknowns; i.e., the n a_k's. This numerical technique guarantees that the residuals of eq A.1 are zero at the collocation points; the n zeros of the nth order Legendre polynomial. Once coefficients a_k are determined, the calculated vapor-phase compositions, y_i(calc), corresponding to the experimental points are obtained from

$$y_i(\text{calc}) = \frac{x_i \gamma_i f_i^o}{\varphi_i p} \quad (A.9)$$

where the activity coefficients γ_i correspond to the exponentials in eq A.1. The whole process of the consistency test is as follows:

1 Obtain an analytical expression for the $p-x$ data. This allows the calculation of (dp/dx) as well as solving eq A.1 at points different from the data points.
2 Calculate V^E, f_i^o, and φ_i as indicated above, using an initial estimate of φ_i equal to unity.
3 Solve eq A.1 for g. This gives the activity coefficients, which are used to calculate the vapor-phase compositions y_i(calc) from eq A.9.
4 Calculate new values of φ_i using y_i(calc) from step 3, and evaluate Henry's constant $H_{1,2}$ from eq A.5. Repeat steps 2 to 4 until successive values of y_i(calc) agree to within 10^{-6}. The end result is a set of γ_i, y_i(calc), and $H_{1,2}$ values that are thermodynamic consistent with the $p-x$ data.
5 Compare the experimental vapor phase compositions with the calculated ones. If the following criterion is satisfied[11]

$$|y_i(\text{calc}) - y_i(\text{exp})| \leq (\Delta x_i + \Delta y_i)$$

where Δx_i and Δy_i are the experimental uncertainties in the liquid and vapor mole fractions, the data point is assumed to be thermodynamically consistent. On the contrary, if

$$|y_i(\text{calc}) - y_i(\text{exp})| > (\Delta x_i + \Delta y_i)$$

the data point is inconsistent, or the methods for calculating fugacities or molar volumes are erroneous.

■ ASSOCIATED CONTENT

Supporting Information. Description of apparatus and uncertainty measurements. This material is available free of charge via the Internet at http://pubs.acs.org.

■ AUTHOR INFORMATION

Corresponding Author

*Tel.: +52 55 9175 6574. E-mail: fgarcias@imp.mx.

Funding Sources

This work was supported by the Mexican Petroleum Institute under Research Projects D.00406 and D.00484.

■ ACKNOWLEDGMENT

The authors would like to acknowledge the contribution of the three anonymous reviewers, whose constructive criticism led to this improved version of the original manuscript.

■ REFERENCES

(1) García-Sánchez, F.; Eliosa-Jiménez, G.; Silva-Oliver, G.; Vázquez-Román, R. Vapor-Liquid Equilibria of Nitrogen-Hydrocarbon Systems Using the PC-SAFT Equation of State. *Fluid Phase Equilib.* **2004**, *217*, 241–253.

(2) Privat, R.; Jaubert, J. N.; Mutelet, F. Addition of the Nitrogen Group to the PPR78 Model (Predictive 1978 Peng Robinson EOS with Temperature-Dependent k_{ij} Calculated through a Group Contribution Method). *Ind. Eng. Chem. Res.* **2008**, *47*, 2033–2048.

(3) Privat, R.; Jaubert, J. N.; Mutelet, F. Use of the PPR78 Model to Predict New Equilibrium Data of Binary Systems Involving Hydrocarbons and Nitrogen. Comparison with Other GCEOS. *Ind. Eng. Chem. Res.* **2008**, *47*, 7483–7489.

(4) van Konynenburg, P. H.; Scott, R. L. Critical Lines and Phase Equilibria in Binary Van der Waals Mixtures. *Philos. Trans. R. Soc. London, Ser. A* **1980**, *298*, 495–540.

(5) Silva-Oliver, G.; Eliosa-Jiménez, G.; García-Sánchez, F.; Avendaño-Gómez, J. R. High-Pressure Vapor-Liquid Equilibria in the Nitrogen-n-Pentane System. *Fluid Phase Equilib.* **2006**, *250*, 37–48.

(6) Eliosa-Jiménez, G.; Silva-Oliver, G.; García-Sánchez, F.; de Ita de la Torre, A. High-Pressure Vapor-Liquid Equilibria in the Nitrogen + n-Hexane System. *J. Chem. Eng. Data* **2007**, *52*, 395–404.

(7) García-Sánchez, F.; Eliosa-Jiménez, G.; Silva-Oliver, G.; Godínez-Silva, A. High-Pressure (Vapor-Liquid) Equilibria in the (Nitrogen + n-Heptane) System. *J. Chem. Thermodyn.* **2007**, *39*, 893–905.

(8) Eliosa-Jiménez, G.; García-Sánchez, F.; Silva-Oliver, G.; Macías-Salinas, R. Vapor-Liquid Equilibrium Data for the Nitrogen + n-Octane System from (344.5 to 543.5) K and at Pressures up to 50 MPa. *Fluid Phase Equilib.* **2009**, *282*, 3–10.

(9) Silva-Oliver, G.; Eliosa-Jiménez, G.; García-Sánchez, F.; Avendaño-Gómez, J. R. High-Pressure Vapor-Liquid Equilibria in the Nitrogen-n-Nonane System. *J. Supercrit. Fluids* **2007**, *42*, 36–47.

(10) García-Sánchez, F.; Eliosa-Jiménez, G.; Silva-Oliver, G.; García-Flores, B. E. Vapor-Liquid Equilibrium Data for the Nitrogen + n-Decane System from (344 to 563) K and at Pressures up to 50 MPa. *J. Chem. Eng. Data* **2009**, *54*, 1560–1568.

(11) Christiansen, L. J.; Fredenslund, A. Thermodynamic Consistency Using Orthogonal Collocation or Computation of Equilibrium Vapor Compositions at High Pressures. *AIChE J.* **1975**, *21*, 49–57.

(12) Peng, D.-Y.; Robinson, D. B. A New Two-Constant Equation of State. *Ind. Eng. Chem. Fundam.* **1976**, *15*, 59–64.

(13) Gross, J.; Sadowski, G. Perturbed-Chain SAFT: An Equation of State Based on Perturbation Theory for Chain Molecules. *Ind. Eng. Chem. Res.* **2001**, *40*, 1244–1260.

(14) Guilbot, P.; Valtz, A.; Legendre, H.; Richon, D. Rapid On-Line Sampler-Injector: a Reliable Tool for HT-HP Sampling and On-Line GC Analysis. *Analusis* **2000**, *28*, 426–431.

(15) Battino, R.; Banzhof, M.; Bogan, M.; Wilhelm, E. Apparatus for Rapid Degassing of Liquids. Part III. *Anal. Chem.* **1971**, *43*, 806–807.

(16) D'Avila, S. G.; Kaul, B. K.; Prausnitz, J. M. Solubilities of Heavy Hydrocarbons in Compressed Methane and Nitrogen. *J. Chem. Eng. Data* **1976**, *21*, 488–491.

(17) Ampueda Ramos, F. Diagrammes de Phases. Hydrocarbures (C_{12})-Fluides Supercritiques (N_2, CO_2, $N_2 + CO_2$). These de Doctorat, Universite Claude-Bernard Lyon I, Lyon, France, 1986.

(18) Llave, F. M.; Chung, T. H. Vapor-Liquid Equilibria of Nitrogen-Hydrocarbon Systems. *J. Chem. Eng. Data* **1988**, *33*, 123–128.

(19) Gao, W.; Robinson, R. L., Jr.; Gasem, K. A. M. High-Pressure Solubilities of Hydrogen, Nitrogen, and Carbon Monoxide in Dodecane from 344 to 410 K at Pressures to 13.2 MPa. *J. Chem. Eng. Data* **1999**, *44*, 130–132.

(20) Frost, A. A.; Kalkwarf, D. R. A Semi-Empirical Equation for the Vapor Pressure of Liquids as a Function of Temperature. *J. Chem. Phys.* **1953**, *21*, 264–267.

(21) Reid, R. C.; Prausnitz, J. M.; Poling, B. E. *The Properties of Gases and Liquids*, 4th ed.; McGraw-Hill: New York, 1987.

(22) Wegstein, J. H. Accelerating Convergence for Iterative Processes. *Commun. Assoc. Comput. Mach.* **1958**, *1*, 9–13.

(23) Won, K. W.; Prausnitz, J. M. High-Pressure Vapor-Liquid Equilibria. Calculation of Partial Pressures from Total Pressure Data. Thermodynamic Consistency. *Ind. Eng. Chem. Fundam.* **1973**, *12*, 459–463.

(24) Villadsen, J.; Stewart, W. E. Solution of Boundary-Value Problems by Orthogonal Collocation. *Chem. Eng. Sci.* **1967**, *22*, 1483–1501.

(25) Michelsen, M. L.; Villadsen, J. A Convenient Computational Procedure for Collocation Constants. *Chem. Eng. J.* **1972**, *4*, 64–68.

(26) Villadsen, J.; Michelsen, M. L. *Solution of Differential Equation Models by Polynomial Approximation*; Prentice-Hall: Englewood Cliffs, NJ, 1978.

(27) Kalra, H.; Robinson, D. B.; Besserer, G. J. The Equilibrium Phase Properties of the Nitrogen-n-Pentane System. *J. Chem. Eng. Data* **1977**, *22*, 215–218.

(28) Justo-García, D. N.; García-Sánchez, F.; Romero-Martinez, A. Isothermal Multiphase Flash Calculations with the PC-SAFT Equation of State. *Am. Inst. Phys. Conf. Proc.* **2008**, *979*, 195–214.

(29) Ambrose, D.; Tsonopoulos, C. Vapor-Liquid Critical Properties of Elements and Compounds. 2. Normal Alkanes. *J. Chem. Eng. Data* **1995**, *40*, 531–546.

(30) Ambrose, D. *Vapour-Liquid Critical Properties*; NPL Report Chemistry 107; National Physical Laboratory: Teddington, 1980.

(31) Nelder, J. A.; Mead, R. A. Simplex Method for Function Minimization. *Comput. J.* **1965**, *7*, 308–313.

(32) Van Ness, H. C. *Classical Thermodynamics of Non-Electrolyte Solutions*; Pergamon Press: Oxford, 1964.

(33) Van Ness, H. C.; Abbott, M. M. *Classical Thermodynamics of Nonelectrolyte Solutions with Applications to Phase Equilibria*; McGraw-Hill: New York, 1982.

(34) Prausnitz, J. M.; Chueh, P. L. *Computer Calculations for High-Pressure Vapor-Liquid Equilibria*; Prentice-Hall: Englewood Cliff, NJ, 1968.

(35) Reid, R. C.; Prausnitz, J. M.; Sherwood, T. K. *The Properties of Gases and Liquids*, 3rd ed.; McGraw-Hill: New York, 1977.

(36) Fredenslund, A. *Thermodynamic Consistency of High-Pressure Vapor-Liquid Equilibrium Data*, Proceedings of the International Symposium on Vapor-Liquid Equilibrium in Multicomponent Systems, Warszawa-Jablonna, November 2−6, 1975.